Exotic bound states of two baryons in light of chiral effective field theory

J. Haidenbauer [a], U.-G. Meißner [a,b]

[a] *Institute for Advanced Simulation, Institut für Kernphysik (Theorie) and Jülich Center for Hadron Physics,*
Forschungszentrum Jülich, D-52425 Jülich, Germany
[b] *Helmholtz-Institut für Strahlen- und Kernphysik (Theorie) and Bethe Center for Theoretical Physics, Universität Bonn,*
D-53115 Bonn, Germany

Abstract

Baryon-baryon bound states in the strangeness $S = -2$, $S = -3$, and $S = -4$ sectors are considered. In particular, the dependence of the corresponding binding energies on the quark mass (or equivalently the pion mass) is explored in the framework of chiral effective field theory, in order to connect with current lattice QCD calculations. For a bound state in the $\Xi\Xi$ $^1S_0$ channel, predicted by our leading-order effective field theory interaction, binding energies are inferred that are roughly in line with a recent lattice QCD result at meson and baryon masses that correspond to those in the lattice simulation. With regard to the so-called H-dibaryon it is shown that the SU(3) breaking effects induced by the differences of the pertinent two-baryon thresholds ($\Lambda\Lambda$, ΞN, $\Sigma\Sigma$) have a very pronounced impact on its binding energy. A bound H-dibaryon as found in two lattice calculations could be shifted above the $\Lambda\Lambda$- or even above the ΞN threshold for physical masses of the involved baryons.

1. Introduction

The term dibaryon is used somewhat ambiguously in the literature. It is applied for single hadrons viewed as genuine compact six-quarks states that are tied together by (rather short-ranged) gluon-exchange forces between the quarks, on one hand side, but also for loosely bound two-baryons systems such as the deuteron, that are formed by long-ranged forces between their constituents. Possibly the most famous one of the former kind is the H-dibaryon which was predicted by Jaffe in 1977 as a deeply bound state with quantum numbers of the $\Lambda\Lambda$ system, i.e. strangeness $S = -2$ and isospin $I = 0$, and with $J^P = 0^+$ [1].

In any case, the aforementioned deuteron (the neutron-proton bound state in the $^3S_1$-$^3D_1$ channel) is so far the only known and unambiguously established dibaryon. The interaction in the $^1S_0$ partial wave of the neutron-proton (np) system is just not strong enough to produce a bound state and only a virtual state is created. Certainly, there is no shortage of new proposals of dibaryon candidates in nucleon-nucleon scattering [2] as well as in the strangeness sector [3]. In particular, the (approximate) SU(3) flavor symmetry of the strong interaction suggests that bound states could exist also in other systems formed by two octet baryons [4]. Indeed meson-exchange models like the Nijmegen baryon-baryon (BB) interaction [5], derived under the assumption of (broken) SU(3) symmetry, predict bound states for the $\Xi\Xi$ but also for the $\Xi\Sigma$

and $\Xi\Lambda$ systems. A BB interaction derived in a rather different way, namely within the framework of chiral effective field theory (EFT) [6,7] generates likewise bound states in the strangeness $S = -3$ and $S = -4$ sectors [8].

With regard to the H-dibaryon, many experimental searches were carried out over the years, but so far no convincing signal was found [9]. Recently, however, the H-dibaryon was put back on the agenda by lattice QCD calculations performed by the NPLQCD [10,11] and HAL QCD [12,13] Collaborations, where evidence for a bound state in the pertinent BB channel was found. The NLPQCD Collaboration reported also evidence for a $\Xi^-\Xi^-$ bound state [11]. Nevertheless, one has to keep in mind that most present-day lattice QCD calculations are not performed at the physical masses of the involved particles. Thus, it is an open question how the binding energies of the calculated states evolve when those masses approach their physical values. Standard chiral extrapolations [14,15] might reach their limits in case of dynamically generated bound states where there is a delicate interplay between the interaction potential (that depends on the pion mass) and the kinetic energy (that is affected by the baryon masses). Specifically in situations where two or more BB channels can couple, as it is the case for the H-dibaryon, the effects due to the baryon masses could be sizeable.

In this paper, we analyze various issues related to lattice QCD calculations in the framework of chiral effective field theory for the BB interaction at leading order (LO) in the Weinberg counting. Indeed, the framework of chiral effective field theory in which our BB interactions are derived is very well suited to shed light on the general characteristics of possible dibaryon bound states and, in particular, to study the quark mass [1] dependence of the binding energies of those states, in complete analogy to calculations of the quark mass dependence of the deuteron binding energy performed in Refs. [16–19]. Another important issue that can be addressed here is how this quark mass dependence is affected when the SU(3) breaking manifested in the masses of the octet baryons is accounted for.

The imposed (approximate) SU(3) flavor symmetry fixes the interactions in the $S = -3$ and $S = -4$ sectors uniquely, once the (five) low-energy constant (LECs) that occur at LO in chiral EFT are determined by a fit to the available hyperon-nucleon data. In particular, our LO interaction published in [6] implies the existence of several bound states in those systems. It will be interesting to see how the corresponding binding energies evolve when we increase the pion mass in order to match with the conditions of present lattice QCD calculations [10–13].

In the $S = -2$ sector with isospin zero where the H-dibaryon is expected there is one additional LEC, corresponding to the SU(3) flavor-singlet channel, that can not be fixed by hyperon-nucleon data. Since the scarce experimental information available for this sector ($\Xi^- p \to \Xi^- p$ and $\Xi^- p \to \Lambda\Lambda$ cross sections [20]) is afflicted with large uncertainties and does not allow to constrain its value [7], one can exploit this freedom and fine-tune the remaining LEC to produce a bound H with a given binding energy, and then study its properties [21]. The case of the H-dibaryon is also very well suited to examine the effects from the SU(3) breaking in the baryon masses because, as said before, for the quantum numbers in question there are three baryon-baryon channels that can couple, namely $\Lambda\Lambda$, ΞN, and $\Sigma\Sigma$. Their physical thresholds are well separated, whereas in a completely SU(3) symmetric world all BB thresholds are degenerate. We will see that this has very definite dynamical consequences.

Our manuscript is organized as follows: In Sec. 2, we recall the basic formalism of the BB interaction in the framework of chiral EFT. Sec. 3 contains a detailed discussion of the quark mass dependence of binding energies in the strangeness $S = -3$ and $S = -4$ sectors, where our chiral EFT interaction but also the meson-exchange potential of the Nijmegen group predict bound states in several BB channels. In Sec. 4 we discuss in detail the situation for the H dibaryon. Specifically, we examine the influence of the SU(3) breaking through the various two-baryon thresholds and we try to make direct contact to the results published by the NPLQCD and HAL QCD Collaborations. The paper ends with some concluding remarks.

---

[1] Because of the Gell-Mann-Oakes-Renner relation, the pion mass squared is proportional to the average light quark mass. Therefore, the notions "quark mass dependence" and "pion mass dependence" can be used synonymously.

	Channel	Isospin	C_{1S0}	Isospin	C_{3S1}
$S=0$	$NN \to NN$	1	C^{27}	0	C^{10^*}
$S=-1$	$\Lambda N \to \Lambda N$	$\frac{1}{2}$	$\frac{1}{10}\left(9C^{27}+C^{8s}\right)$	$\frac{1}{2}$	$\frac{1}{2}\left(C^{8a}+C^{10^*}\right)$
	$\Lambda N \to \Sigma N$	$\frac{1}{2}$	$\frac{3}{10}\left(-C^{27}+C^{8s}\right)$	$\frac{1}{2}$	$\frac{1}{2}\left(-C^{8a}+C^{10^*}\right)$
	$\Sigma N \to \Sigma N$	$\frac{1}{2}$	$\frac{1}{10}\left(C^{27}+9C^{8s}\right)$	$\frac{1}{2}$	$\frac{1}{2}\left(C^{8a}+C^{10^*}\right)$
	$\Sigma N \to \Sigma N$	$\frac{3}{2}$	C^{27}	$\frac{3}{2}$	C^{10}
$S=-2$	$\Lambda\Lambda \to \Lambda\Lambda$	0	$\frac{1}{40}\left(27C^{27}+8C^{8s}+5C^1\right)$		
	$\Lambda\Lambda \to \Xi N$	0	$\frac{-1}{40}\left(18C^{27}-8C^{8s}-10\,C^1\right)$		
	$\Lambda\Lambda \to \Sigma\Sigma$	0	$\frac{\sqrt{3}}{40}\left(-3C^{27}+8C^{8s}-5C^1\right)$		
	$\Xi N \to \Xi N$	0	$\frac{1}{40}\left(12C^{27}+8C^{8s}+20\,C^1\right)$	0	C^{8a}
	$\Xi N \to \Sigma\Sigma$	0	$\frac{\sqrt{3}}{40}\left(2C^{27}+8C^{8s}-10\,C^1\right)$	1	$\frac{\sqrt{2}}{6}\left(C^{10}+C^{10^*}-2C^{8a}\right)$
	$\Sigma\Sigma \to \Sigma\Sigma$	0	$\frac{1}{40}\left(C^{27}+24C^{8s}+15C^1\right)$	1	$\frac{1}{6}\left(C^{10}+C^{10^*}+4C^{8a}\right)$
	$\Xi N \to \Xi N$	1	$\frac{1}{5}\left(2C^{27}+3C^{8s}\right)$	1	$\frac{1}{3}\left(C^{10}+C^{10^*}+C^{8a}\right)$
	$\Xi N \to \Sigma\Lambda$	1	$\frac{\sqrt{6}}{5}\left(C^{27}-C^{8s}\right)$	1	$\frac{\sqrt{6}}{6}\left(C^{10}-C^{10^*}\right)$
	$\Sigma\Lambda \to \Sigma\Lambda$	1	$\frac{1}{5}\left(3C^{27}+2C^{8s}\right)$	1	$\frac{1}{2}\left(C^{10}+C^{10^*}\right)$
	$\Sigma\Lambda \to \Sigma\Sigma$			1	$\frac{\sqrt{3}}{6}\left(C^{10}-C^{10^*}\right)$
	$\Sigma\Sigma \to \Sigma\Sigma$	2	C^{27}		
$S=-3$	$\Xi\Lambda \to \Xi\Lambda$	$\frac{1}{2}$	$\frac{1}{10}\left(9C^{27}+C^{8s}\right)$	$\frac{1}{2}$	$\frac{1}{2}\left(C^{8a}+C^{10}\right)$
	$\Xi\Lambda \to \Xi\Sigma$	$\frac{1}{2}$	$\frac{3}{10}\left(-C^{27}+C^{8s}\right)$	$\frac{1}{2}$	$\frac{1}{2}\left(-C^{8a}+C^{10}\right)$
	$\Xi\Sigma \to \Xi\Sigma$	$\frac{1}{2}$	$\frac{1}{10}\left(C^{27}+9C^{8s}\right)$	$\frac{1}{2}$	$\frac{1}{2}\left(C^{8a}+C^{10}\right)$
	$\Xi\Sigma \to \Xi\Sigma$	$\frac{3}{2}$	C^{27}	$\frac{3}{2}$	C^{10^*}
$S=-4$	$\Xi\Xi \to \Xi\Xi$	1	C^{27}	0	C^{10}

Table 1

Various LO baryon-baryon contact potentials for the $^1S_0$ and $^3S_1$ partial waves in the isospin basis. C^{27} etc. refers to the corresponding $SU(3)_f$ irreducible representation.

2. The baryon-baryon interaction to leading order

For details on the derivation of the chiral BB potentials for the strangeness sector at LO using the Weinberg power counting, we refer the reader to Refs. [6,7,22], see also Refs. [23–25]. Here, we just briefly summarize the basic ingredients of the chiral EFT for BB interactions.

The LO potential consists of four-baryon contact terms without derivatives and of one-pseudoscalar-meson exchanges. The LO $SU(3)_f$ invariant contact terms for the octet BB interactions that are Hermitian and invariant under Lorentz transformations follow from the Lagrangians

$$\mathcal{L}^1 = C_i^1 \left\langle \bar{B}_a \bar{B}_b \left(\Gamma_i B\right)_b \left(\Gamma_i B\right)_a \right\rangle , \quad \mathcal{L}^2 = C_i^2 \left\langle \bar{B}_a \left(\Gamma_i B\right)_a \bar{B}_b \left(\Gamma_i B\right)_b \right\rangle ,$$
$$\mathcal{L}^3 = C_i^3 \left\langle \bar{B}_a \left(\Gamma_i B\right)_a \right\rangle \left\langle \bar{B}_b \left(\Gamma_i B\right)_b \right\rangle . \tag{1}$$

Here a, b denote the Dirac indices of the particles, B is the irreducible octet (matrix) representation of $SU(3)_f$, and the Γ_i are the usual elements of the Clifford algebra [6]. As described in Ref. [6], to LO the Lagrangians in Eq. (1) give rise to only six independent low-energy constants (LECs), the C_i^j in Eq. (1), due to $SU(3)_f$ constraints. They need to be determined by a fit to experimental data. It is convenient to re-express the BB potentials in terms of the $SU(3)_f$ irreducible representations, see e.g. Refs. [26,27]. Then the contact interaction is given by

$$V = \frac{1}{4}(1 - \boldsymbol{\sigma}_1 \cdot \boldsymbol{\sigma}_2)\, C_{1S0} + \frac{1}{4}(3 + \boldsymbol{\sigma}_1 \cdot \boldsymbol{\sigma}_2)\, C_{3S1} , \tag{2}$$

and the constraints imposed by the assumed $SU(3)_f$ symmetry on the interactions in the various BB channels for the $^1S_0$ and $^3S_1$ partial waves can be readily read off from Table 1.

The lowest order $SU(3)_f$ invariant pseudoscalar-meson–baryon interaction Lagrangian embodying the appropriate symmetries was also discussed in [6]. The invariance under $SU(3)_f$ transformations implies specific relations between the various coupling constants, namely

$$f_{NN\pi} = f, \qquad f_{NN\eta_8} = \frac{1}{\sqrt{3}}(4\alpha - 1)f, \quad f_{\Lambda NK} = -\frac{1}{\sqrt{3}}(1 + 2\alpha)f,$$

$$f_{\Xi\Xi\pi} = -(1 - 2\alpha)f, \quad f_{\Xi\Xi\eta_8} = -\frac{1}{\sqrt{3}}(1 + 2\alpha)f, \quad f_{\Xi\Lambda K} = \frac{1}{\sqrt{3}}(4\alpha - 1)f,$$

$$f_{\Lambda\Sigma\pi} = \frac{2}{\sqrt{3}}(1 - \alpha)f, \quad f_{\Sigma\Sigma\eta_8} = \frac{2}{\sqrt{3}}(1 - \alpha)f, \quad f_{\Sigma NK} = (1 - 2\alpha)f, \tag{3}$$

$$f_{\Sigma\Sigma\pi} = 2\alpha f, \qquad f_{\Lambda\Lambda\eta_8} = -\frac{2}{\sqrt{3}}(1 - \alpha)f, \quad f_{\Xi\Sigma K} = -f.$$

Here $f \equiv g_A/2F_\pi$, where g_A is the nucleon axial-vector strength and F_π is the weak pion decay constant. We use the values $g_A = 1.26$ and $F_\pi = 92.4$ MeV. For α, the $F/(F + D)$-ratio [6], we adopt the SU(6) value: $\alpha = 0.4$, which is consistent with recent determinations of the axial-vector coupling constants [28,29].

The spin-space part of the LO one-pseudoscalar-meson-exchange potential is similar to the static one-pion-exchange potential in chiral EFT for nucleon-nucleon interactions, see e.g. [30] (recoil and relativistic corrections give higher order contributions),

$$V^{B_1 B_2 \to B_1' B_2'} = -f_{B_1 B_1' P} f_{B_2 B_2' P} \frac{(\boldsymbol{\sigma}_1 \cdot \mathbf{q})(\boldsymbol{\sigma}_2 \cdot \mathbf{q})}{\mathbf{q}^2 + M_P^2}, \tag{4}$$

where M_P is the mass of the exchanged pseudoscalar meson. The transferred momentum $\mathbf{q}$ is defined in terms of the final and initial center-of-mass (c.m.) momenta of the baryons, $\mathbf{p}'$ and $\mathbf{p}$, as $\mathbf{q} = \mathbf{p}' - \mathbf{p}$. In the calculation we use the (isospin averaged) physical masses of the exchanged pseudoscalar mesons, i.e. $M_\pi = 138.04$ MeV, $M_K = 495.66$ MeV, and $M_\eta = 548.8$ MeV. The explicit SU(3) breaking reflected in the mass splitting between the pseudoscalar mesons and, in particular, the small mass of the pion relative to the other members of the octet leads to sizeable differences in the range of the interactions in the different channels and, thus, induces an essential dynamical breaking of SU(3) symmetry in the BB interactions. The η meson was identified with the octet η (η_8) and its physical mass was used. Note that for getting the actual potential for a specific channel one still has to multiply the expression in Eq. (4) with the pertinent isospin coefficient (as given, e.g., in Ref. [6]).

The reaction amplitudes are obtained from the solution of a coupled-channel Lippmann-Schwinger (LS) equation for the interaction potentials:

$$T^{\nu''\nu',J}_{\rho''\rho'}(p'', p'; \sqrt{s}) = V^{\nu''\nu',J}_{\rho''\rho'}(p'', p') + \sum_{\rho,\nu} \int_0^\infty \frac{dp\,p^2}{(2\pi)^3} V^{\nu''\nu,J}_{\rho''\rho}(p'', p) \frac{2\mu_\nu}{q_\nu^2 - p^2 + i\eta} T^{\nu\nu',J}_{\rho\rho'}(p, p'; \sqrt{s}). \tag{5}$$

The label ν indicates the particle channels and the label ρ the partial wave. μ_ν is the pertinent reduced mass. The on-shell momentum in the intermediate state, q_ν, is defined by $\sqrt{s} = \sqrt{m_{B_{1,\nu}}^2 + q_\nu^2} + \sqrt{m_{B_{2,\nu}}^2 + q_\nu^2}$. Relativistic kinematics is used for relating the laboratory energy T_{lab} of the hyperons to the c.m. momentum.

In [6,7] the LS equation was solved in the particle basis, in order to incorporate the correct physical thresholds. Since here we are primarily interested in bound states we work in the isospin basis. Furthermore, we ignore the Coulomb interaction (as it is also done in the pertinent lattice QCD calculations). We use the following (isospin averaged) baryon masses: $m_N = 939.6$ MeV, $m_\Lambda = 1115.6$ MeV, $m_\Sigma = 1192.5$ MeV, and $m_\Xi = 1318.1$ MeV. In the $S = -4$ and $S = -3$ sectors either single channel ($\Xi\Xi$) or coupled-channel ($\Xi\Lambda - \Xi\Sigma$) equations have to be solved. For $S = -2$ and, in particular, for the H-dibaryon there are three coupled channels, namely $\Lambda\Lambda$, ΞN and $\Sigma\Sigma$. The potentials in the LS equation are cut off with a regulator function, $\exp\left[-\left(p'^4 + p^4\right)/\Lambda^4\right]$, in order to remove high-energy components of the baryon and pseudoscalar meson fields [31]. We consider cut-off values in the range from 550 to 700 MeV, similar to what was used for chiral NN potentials [31].

The imposed SU(3) flavor symmetry implies that only five of the six LECs contribute to the YN interaction, namely C^{27}, C^{10}, C^{10^*}, C^{8_s}, and C^{8_a}, cf. Table 1. These five contact terms were determined in [6] by a fit to the YN scattering data. Since the NN data cannot be described with a LO EFT (except very close to the threshold), SU(3) constraints from the NN interaction were not implemented explicitly. As shown in Ref. [6], a good description of the 35 low-energy YN scattering can be obtained for cutoff values $\Lambda = 550, ..., 700$ MeV and for natural values of the LECs. The sixth LEC (C^1) is only present in the

$S = -2$ channels with isospin zero, cf. Table 1. There is scarce experimental information on these channels that could be used to fix this LEC, but it turned out that the quality of the existing data does not really allow to constrain its value reliably [7]. Even with the value of the sixth LEC chosen so that $C_{1S0}^{\Lambda\Lambda\to\Lambda\Lambda} = 0$, agreement with those data can be achieved. In this case a scattering length of $a_{1S_0}^{\Lambda\Lambda} = -1.52$ fm [7] is obtained. Analyses of the measured binding energy of the double-strange hypernucleus $_{\Lambda\Lambda}^{6}$He [32] suggest that the $\Lambda\Lambda$ scattering length could be in the range of -1.3 to -0.7 fm [33–35]. A first determination of the scattering length utilizing data on the $\Lambda\Lambda$ invariant mass from the reaction $^{12}C(K^-, K^+\Lambda\Lambda X)$ led to the result $a^{\Lambda\Lambda} = -1.2 \pm 0.6$ fm [36].

3. Quark mass dependence of baryon-baryon binding energies

As discussed in Ref. [8], our LO chiral EFT interaction predicts several bound states for the strangeness $S = -3$ and $S = -4$ sectors. Let us start with the $^1S_0$ partial wave in the $\Xi^0\Lambda$ channel. For the smallest cut-off ($\Lambda = 550$ MeV) only a virtual state is found in this partial wave which, however, eventually transforms into a real bound state when the cut-off is increased within the considered range. For the largest cut-off (700 MeV) a binding energy of -0.43 MeV is predicted. The results for the $\Xi^0\Lambda$ channel of other potentials that provide detailed results for the $S = -3$ and $S = -4$ sectors [5,35] suggest also an overall attractive interaction in the $^1S_0$ partial wave though only a very moderate one which does not support a bound state. The S-waves in the $\Xi\Sigma$ $I = 3/2$ channel belong to the same (10^* and 27, respectively, cf. Table 1) irreducible representations where in the NN case bound states ($^3S_1$-$^3D_1$) or virtual states ($^1S_0$) exist. Therefore, one expects that such states can also occur for $\Xi\Sigma$. Indeed, here bound states are present for both partial waves in the Nijmegen model, cf. the discussion in Sect. III.B in Ref. [5]. The chiral EFT interaction has a bound state too for $^1S_0$, for all cut-off values [8]. The binding energies lie in the range of -2.23 MeV ($\Lambda = 550$ MeV) to -6.15 MeV (700 MeV). But in the $^3S_1$-$^3D_1$ partial wave the attraction is obviously not strong enough to form a bound state. The $^1S_0$ state of the $\Xi\Xi$ channel belongs also to the 27plet irreducible representation and also here the Nijmegen as well as the chiral EFT interactions produce bound states. In our case the binding energy lies in the range of -2.56 MeV ($\Lambda = 550$ MeV) to -7.28 MeV (700 MeV).

Since the $^1S_0$ partial waves in the ΣN ($I = 3/2$) and $\Sigma\Sigma$ ($I = 2$) channels belong likewise to the 27plet, cf. Table 1, one could expect bound states in those states, too. However, our chiral EFT interaction is only moderately attractive in the former case, as reflected in the corresponding scattering lengths which range from -2.24 to -2.36 fm, cf. [6]. There is also no bound state for $\Sigma^+\Sigma^+$, though the predicted scattering lengths are here between -6.23 to -9.42 fm, which is an indication that there is a virtual state not too far from the physical region. Note that in our calculation $\Sigma\Sigma\,(I = 2) \equiv \Sigma^+\Sigma^+ \equiv \Sigma^-\Sigma^-$ and, therefore, we use those designations synonymously here. The Nijmegen NSC97 potential, on the other hand, clearly produces a bound state in the $\Sigma^+\Sigma^+$ state, as signalled by the large and positive scattering lengths [5]. Interestingly, a BB interaction derived within the constituent quark-model (fss2) [35], yields also a scattering length that is very large and negative so that there should be a virtual state practically at the $\Sigma^+\Sigma^+$ threshold. On the other hand, for all $S = -3$ and $S = -4$ partial waves no bound states are predicted by this interaction model based on quark-gluon dynamics [35].

Let us now consider variations of the masses of the involved particles. First we study the dependence of the binding energies on the pion mass M_π and keep the baryon masses at their physical values. We will examine the specific situation for the concrete (meson and baryon) masses that correspond to the calculation reported by the NPLQCD Collaboration below.

Our results are displayed in Figs. 1 and 2. Obviously for the $S = -3$ and $S = -4$ systems (Fig. 1) there is a fairly weak dependence of the predicted binding energies on the pion mass. In particular, the variation from the physical point to masses around 400 MeV, corresponding to the present status of the NPLQCD computations, are relatively small compared to the differences due to the cut-off variations. Note that for $\Xi\Sigma$ the binding energy decreases with increasing pion mass, in contrast to what happens in the other channels.

Results for the $S = -1$ and $S = -2$ systems are presented in Fig. 2. Contrary to the $\Lambda\Lambda$ system, which we discuss in the next section, the $\Sigma\Sigma$ interaction in the $I = 2$ channel is completely fixed by the five LECs that
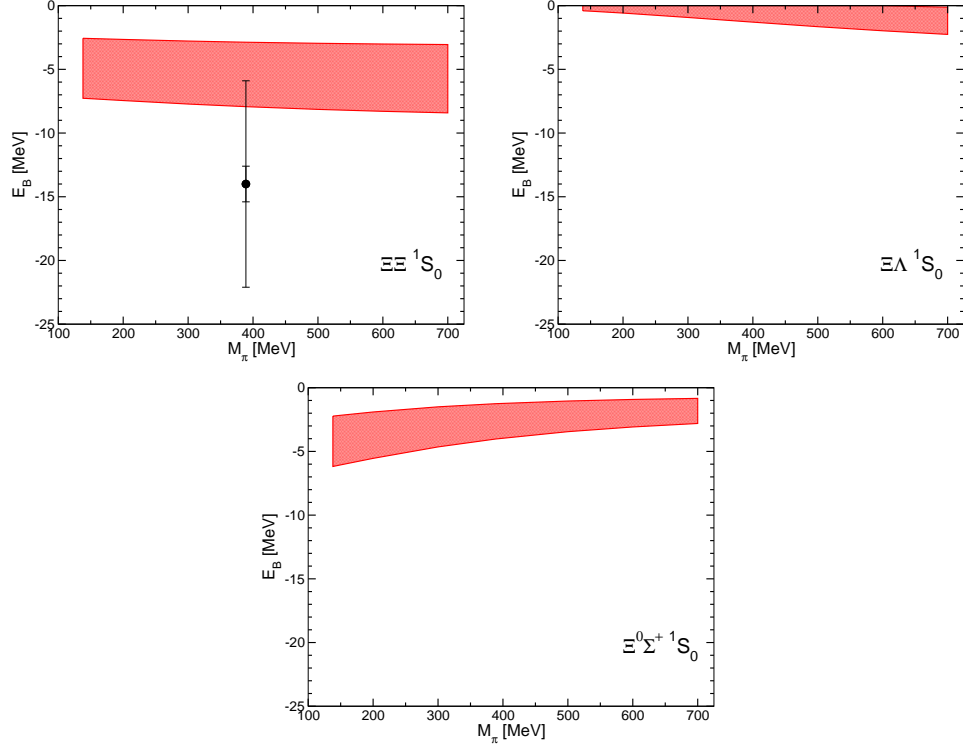
Fig. 1. Dependence of the binding energies in different $S = -3$ and $S = -4$ $^1S_0$ partial waves on the pion mass.

could be determined by a fit to the YN data, cf. Table 1. Thus predictions can be made for this system too. Interestingly, while being unbound at the physical point, a bound $\Sigma^+\Sigma^+$ state is created when the pion mass is increased. For $M_\pi \approx 400$ MeV the predicted binding energy is around 2-3 MeV. Note that corresponding investigations within lattice QCD remained inconclusive in this case [11]. A bound state appears too in the Σ^+p system, however, only for pion masses above 400 MeV. Note that $\Sigma N\,(I = 3/2) \equiv \Sigma^+p \equiv \Sigma^-n$. For both systems we observe a somewhat stronger dependence of the binding energies on the pion mass as compared to $S = -3$ and $S = -4$.

The dependence on the pion mass can be easily understood, on a qualitative level, by considering the contributions from pseudoscalar-meson exchange to the interaction in the various baryon-baryon systems. Though in a fully SU(3) symmetric world

$$V^{NN \to NN}_{(I=1)} = V^{\Sigma N \to \Sigma N}_{(I=3/2)} = V^{\Sigma\Sigma \to \Sigma\Sigma}_{(I=2)} = V^{\Xi\Sigma \to \Xi\Sigma}_{(I=3/2)} = V^{\Xi\Xi \to \Xi\Xi}_{(I=1)} = V^{27} \qquad (6)$$

in the $^1S_0$ partial wave, one has to keep in mind that the indivudal contributions of the pseudoscalar mesons differ for different channels. Their relative strengths in the various channels follows from the product of the relevant coupling constants, fixed by the assumed SU(3) symmetry, which are tabulated in Eq. (3), and a corresponding isospin factor:

$$
\begin{array}{llll}
NN \to NN: & V_\pi \propto f^2, & V_\eta \propto (3/25) \times f^2 & \\
\Sigma N \to \Sigma N: & V_\pi \propto (20/25) \times f^2, & V_\eta \propto (6/25) \times f^2, & V_K \propto (2/25) \times f^2 \\
\Sigma\Sigma \to \Sigma\Sigma: & V_\pi \propto (16/25) \times f^2, & V_\eta \propto (12/25) \times f^2 & \\
\Xi\Sigma \to \Xi\Sigma: & V_\pi \propto (-4/25) \times f^2, & V_\eta \propto (-18/25) \times f^2, & V_K \propto 2 \times f^2 \\
\Xi\Xi \to \Xi\Xi: & V_\pi \propto (1/25) \times f^2, & V_\eta \propto (27/25) \times f^2 &
\end{array}
\qquad (7)
$$

Let us compare, for example, NN and $\Xi\Xi$. Obviously in the NN case the pion-exchange contribution dominates while for $\Xi\Xi$ practically the whole contribution from pseudoscalar-meson exchange is due to the η
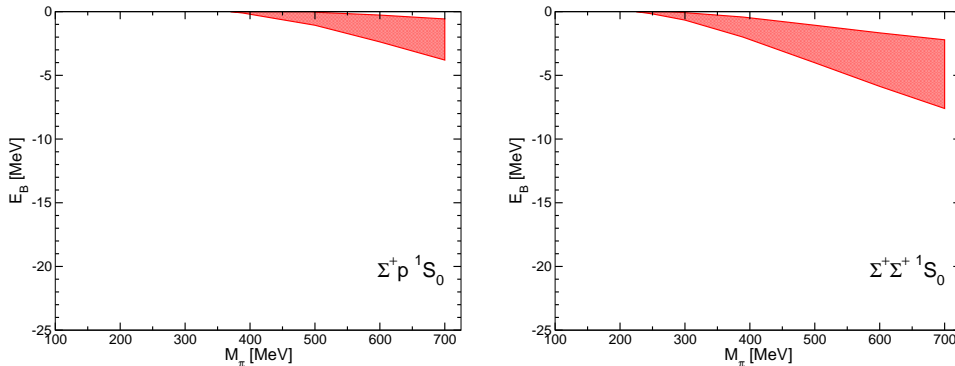
Fig. 2. Dependence of the binding energies in the $\Sigma^+ p$ (left) and $\Sigma^+ \Sigma^+$ (right) $^1S_0$ partial waves on the pion mass.

meson. Consequently, variations of the pion mass (or the SU(3) breaking manifested by the small pion mass) are much less important for the $\Xi\Xi$ system than for the NN interaction, cf. Refs. [16–19] for a discussion of the effects in the latter system. Since the small value $f_{\Xi\Xi\pi} = -0.2 \times f$ enters also into the $\Xi\Sigma$ interaction a similarly weak dependence is seen there. Note that $V_\pi^{\Xi\Sigma\to\Xi\Sigma} = -4 \times V_\pi^{\Xi\Xi\to\Xi\Xi}$ for the isospin channels shown in Fig. 1, which explains the opposite trend in the dependence of the binding energy on the pion mass. In case of $\Xi\Lambda$, pion-exchange contributes only via coupled-channel effects so that one expects a weak pion-mass dependence anyway. In the channels ΣN and $\Sigma\Sigma$ where the strength of pion exchange is less reduces as compared to NN ($V_\pi^{\Sigma N\to\Sigma N} = 4/5 \times V_\pi^{NN\to NN}$, $V_\pi^{\Sigma\Sigma\to\Sigma\Sigma} = 16/25 \times V_\pi^{NN\to NN}$) we observe a sizeable pion mass dependence of the binding energies, cf. Fig. 2. Similar comments also apply for the pion mass dependence of the baryon octet states with increasing strangeness [37]. Note that the relations in Eq. (7) follow for the SU(6) value $\alpha = 0.4$, but they change only marginally for values of $\alpha \approx 0.36 - 0.37$, as determined recently in analyses of hyperon semi-leptonic decay data [28,29].

In order to connect as closely as possible to the results published by the NPLQCD Collaboration [38] we performed also calculations with meson and baryon masses corresponding precisely to those in the lattice QCD simulation. Specifically, we use $M_\pi = 389$ MeV, $M_K = 544$ MeV, and $M_\eta = 587$ MeV, and the baryon masses $m_N = 1151.3$ MeV, $m_\Lambda = 1241.9$ MeV, $m_\Sigma = 1280.3$ MeV, and $m_\Xi = 1349.6$ MeV, all taken from Ref. [38]. Corresponding results are summarized in Table 2 where we also include the binding energies at the physical point and those where only the pion mass was set to $M_\pi = 389$ MeV. All values are given with two digits behind the comma in order to facilitate an easy comparison of the relative size of the various effects. The absolute uncertainty of our leading-order calculation is, of course, best reflected in the cut-off dependence of the results represented by the shaded bands in Figs. 1 and 2 and by the pertinent values in Table 2.

The results in Table 2 make clear that there are sizeable effects from the baryon masses (and of the heavy pseudoscalar mesons K and η, too) on the binding energies. Specifically in the $S = -3$ and $S = -4$ sectors those are more significant than the variations in the pion mass that we considered, which is not surprising if one recalls the discussion above. Clearly, one has to acknowledge that the systematic uncertainty in the current lattice QCD calculations is still significantly larger than those mass effects [11]. Despite of this, it is remarkable that the $\Xi^-\Xi^-$ binding energy published in [11], $E_B = (-14.0 \pm 1.4 \pm 6.7)$ MeV, is rather well in line with the corresponding predictions based on LO chiral EFT. Considering the (rather modest) mass dependence found in our calculation we would expect that this state is still bound at the physical point, namely by roughly 10 MeV if one takes the central value from [11] as guideline. Future lattice QCD calculations with improved statistics will certainly resolve this exciting issue, once the systematic uncertainties can be reduced.

With regard to the other states listed in Table 2 only the one in the $\Xi^-\Sigma^-$ $^1S_0$ partial wave is likely to survive for physical masses. All other states are fairly loosely bound already for masses corresponding to the NPLQCD calculation and disappear when we go to the physical point.

In this context let us emphasize that, of course, it would be also interesting to confirm or exclude the

	χEFT			NPLQCD [11]
	physical masses	$M_\pi = 389$ MeV	NPLQCD masses	
Λ [MeV]	$550 \cdots 700$	$550 \cdots 700$	$550 \cdots 700$	
$\Xi^-\Xi^-$	$-2.56 \cdots -7.27$	$-2.87 \cdots -7.93$	$-3.92 \cdots -10.41$	-14.0 ± 1.4 ± 6.7
$\Xi^-\Lambda$	$0 \cdots -0.40$	$0 \cdots -1.26$	$-1.05 \cdots -4.86$	
$\Xi^-\Sigma^-$	$-2.23 \cdots -6.18$	$-1.25 \cdots -4.02$	$-2.89 \cdots -7.93$	
$\Sigma^-\Sigma^-$	–	$-0.42 \cdots -1.99$	$-1.23 \cdots -3.93$	inconclusive
$\Sigma^- n$	–	$0 \cdots -0.11$	$-0.30 \cdots -1.56$	

Table 2
Binding energies in MeV of various BB bound states in the $^1S_0$ partial wave as obtained from the EFT potential for physical masses (second column), for a pion mass of $M_\pi = 389$ MeV (third column), and using meson and baryon masses that correspond to the lattice QCD calculation of [11] (fourth column). The last column are results of the lattice QCD calculation taken from Ref. [11].

existence of those bound states experimentally. The possibility to find signals for strange di-baryon states in heavy-ion collisions was discussed in Refs. [39,40]. Also the new facilities J-PARC (Tokai, Japan) and FAIR (Darmstadt, Germany) could allow one to obtain empirical constraints on the baryon-baryon interaction in the $S = -3$ and -4 sector. Information could come from formation experiments of corresponding hypernuclei or from proton-proton and antiproton-proton collisions at such high energies that pairs of baryons with strangeness $S = -3$ or $S = -4$ can be produced.

4. The H-dibaryon

4.1. General considerations

As already said, in the $S = -2$ sector with isospin zero where the H-dibaryon is expected there is one additional contact term (C^1, cf. Table 1), corresponding to the SU(3) flavor-singlet channel, that is not fixed by hyperon-nucleon data and, therefore, no immediate predictions can be made. In principle, this LEC could be determined from experimental information available for this sector, but the scarce data ($\Xi^- p \to \Xi^- p$ and $\Xi^- p \to \Lambda\Lambda$ cross sections [20]) are afflicted with large uncertainties and do not allow to constrain its value [7]. Thus, in practice one can exploit this freedom and fine-tune the remaining LEC to produce a bound H with a given binding energy, and then study its properties [21]. Indeed, it turned out that a near-threshold bound state can be easily produced for C^1 values that are of natural size.

In the following we assume that the H-dibaryon is a (loosely) bound BB state [21], just like the bound states discussed in the previous section. We do not consider the case where the H-dibaryon is a genuine 6-quark state as originally suggested by Jaffe [1]. In fact, we cannot say anything about the latter situation within our framework. We also assume that the binding energy, E_H, is similar to that of the deuteron (D) because this allows us to compare the properties of the generated H-dibaryon directly with the familiar deuteron case. Specifically, we fix the value of the flavor-singlet LEC C^1 in such a way that the binding momentum is $\gamma_H = \gamma_D = 0.23161$ fm ($E = -\gamma^2/m_B$, where m_B is either m_N or m_Λ), in view of the well-known relation between the binding energy and the effective range parameters [41,42]

$$\frac{1}{a} \simeq \gamma - \frac{1}{2}r\gamma^2.$$

This relation is very well fulfilled for the deuteron and the corresponding neutron-proton $^3S_1$ scattering length ($a = 5.43$ fm) and effective range ($r = 1.76$ fm). One would naively expect that the same should happen for the H-dibaryon. However, it turns out that the corresponding results for $\Lambda\Lambda$ in the $^1S_0$ partial wave are quite different, namely $a = 3.00$ fm and $r = -4.95$ fm. Specifically, the effective range is much larger and, moreover, negative. Clearly, the properties of the H-dibaryon are not comparable to those of the deuteron, despite the fact that both bound states are close to the elastic threshold. Indeed, if one recalls the expressions for the relevant potentials as given in Table 1,
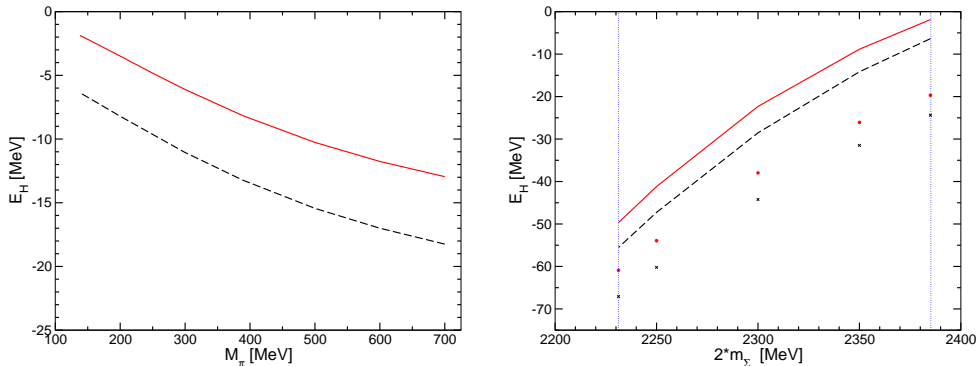
Fig. 3. Dependence of the binding energy of the H-dibaryon on the pion mass M_π (left) and on the Σ mass m_Σ (right). The solid curve correspond to the case where C^1 is fixed such that $E_H = -1.87\,\text{MeV}$ for physical masses while for the dashed curve C^1 is fixed to yield $E_H = -13.2\,\text{MeV}$ for $M_\pi = 389$ MeV. The asterisks and crosses represent results where, besides the variation of m_Σ, $m_\Xi + m_N = 2m_\Lambda$ is assumed so that the ΞN threshold coincides with that of the $\Lambda\Lambda$ channel. The vertical (dotted) lines indicate the physical $\Lambda\Lambda$ and $\Sigma\Sigma$ thresholds.

$$V^{\Lambda\Lambda\to\Lambda\Lambda} = \frac{1}{40}\left(27C^{27} + 8C^{8_s} + 5C^1\right), \quad V^{\Xi N\to\Xi N} = \frac{1}{40}\left(12C^{27} + 8C^{8_s} + 20C^1\right),$$

one can see that the attraction provided by the SU(3) flavor-singlet state (i.e. C^1) contributes with a much larger weight to the ΞN channel than to $\Lambda\Lambda$. This indicates that the presumed H-dibaryon could be predominantly a ΞN bound state. We have confirmed this conjecture by evaluating explicitly the phase shifts in the $\Lambda\Lambda$ and ΞN channels, cf. the discussion in the next section. Indeed, one finds that the phase shift for the ΞN channel is rather similar to the $NN\,^3S_1$ case. Specifically, the ΞN ($^1S_0$) phase shift $\delta(q_{\Xi N})$ fulfills $\delta(0) - \delta(\infty) = 180°$ in agreement with the Levinson theorem. The $\Lambda\Lambda$ ($^1S_0$) phase behaves rather differently and satisfies $\delta(q_{\Lambda\Lambda} = 0) - \delta(\infty) = 0$. Note that there have been earlier discussions on this issue in the context of $S = -2$ baryon-baryon interactions derived within the quark model [43,44].

The results above were obtained with the LECs C^{27} and C^{8_s} fixed from the YN data for the cutoff value $\Lambda = 550$ MeV [6]. We considered also the other variants corresponding to cutoff masses of 600, 650, and 700 MeV in the LS equation (5), as in Ref. [7]. But since the contact term C^1 has to be determined anew in each case it turned out that the results are rather similar for all cutoffs once C^1 is fixed in such a way that the same binding energy for the H dibaryon is produced. Thus, we will present only results for the $\Lambda = 550$ MeV case. We denote the YY interaction with a loosely bound H dibaryon by YY-D in the following, and use the notation YY(550) for the original interaction from Ref. [7].

Let us now consider variations of the masses of the involved particles. The dependence of the H binding energy on the pion mass M_π is displayed in Fig. 3 (left). For the YY-D potential considered above, enlarging the pion mass to around 400 MeV (i.e. to values in an order that corresponds to the NPLQCD calculation [10]) increases the binding energy to around 8 MeV and a further change of M_π to 700 MeV (corresponding roughly to the HAL QCD calculation [12]) yields then 13 MeV, cf. the solid line. Readjusting C^1 so that we predict a H binding energy of 13.2 MeV for $M_\pi = 389$ MeV, corresponding to the latest result published by NPLQCD [11], yields the dashed curve. It is obvious that the dependence on M_π we obtain agrees – at least on a qualitative level – with that presented in Ref. [14]. Specifically, our calculation exhibits the same trend (a decrease of the binding energy with decreasing pion mass) and our binding energy of 9 MeV at the physical pion mass is within the error bars of the results given in [14]. On the other hand, we clearly observe a non-linear dependence of the binding energy on the pion mass. As a consequence, scaling our results to the binding energy reported by the HAL QCD Collaboration [12] (30-40 MeV for $M_\pi \approx 700 - 1000$ MeV) yields binding energies of more than 20 MeV at the physical point, which is certainly outside of the range suggested in Ref. [14]. However, we note that for such large pion masses the LO chiral EFT can not be trusted quantitatively. We remark that in our simulations the curves corresponding to different binding energies remained roughly parallel even up to such large values as suggested by the HAL QCD Collaboration.

Our finding that any H-dibaryon is very likely a bound ΞN state rather than a $\Lambda\Lambda$ state, which follows

9

from the assumed (approximate) SU(3) symmetry of the interaction, suggests that not only the pion mass but also the masses of the baryons play a significant role for the concrete value of binding energy. In the specific case of $J = 0$, $I = 0$, $S = -2$ we are dealing with three coupled channels, namely $\Lambda\Lambda$, ΞN, and $\Sigma\Sigma$. For the isospin-averaged masses that we use their thresholds are at 2231.2, 2257.7, and 2385.0 MeV, respectively. Thus, the physical difference between the $\Lambda\Lambda$ and ΞN thresholds of around 26 MeV implies that the H-dibaryon considered above is, in reality, bound by roughly 28 MeV with respect to its "proper" threshold. Accordingly, one intuitively expects that in a fully SU(3) symmetric case, where the masses of all octet baryons coincide, the bound state would remain more or less fixed to the ΞN threshold and then would lie also about 28 MeV below the $\Lambda\Lambda$ threshold. Since we know from our experience with coupled-channel problems [6,8,45,46] that coupling effects are sizeable and the actual separation of the various thresholds plays a crucial role we investigated also the dependence of the H binding energy on the thresholds (i.e. on the Σ, and on the Ξ and N masses). Corresponding results are displayed in Fig. 3 in the right panel.

We start with considering the effect of the $\Sigma\Sigma$ channel because its threshold is separated by roughly 154 MeV from the one of $\Lambda\Lambda$ so that there is a rather drastic breaking of the SU(3) symmetry. Indeed, when we decrease the Σ mass so that the nominal $\Sigma\Sigma$ threshold (at 2385 MeV) moves downwards and finally coincides with the one of the $\Lambda\Lambda$ channel (2231.2 MeV), we observe a concurrent fairly drastic increase in the H binding energy, cf. the solid curve in Fig. 3 for results based on the interaction YY-D with a binding energy of -1.87 MeV for physical masses of the mesons and baryons. In this context we want to point out that the direct interaction in the $\Sigma\Sigma$ channel is actually repulsive for the low-energy coefficients C^{27} and C^{8_s} fixed from the YN data plus the pseudoscalar meson exchange contributions with coupling constants determined from the SU(3) relations Eq. (3), and it remains repulsive even for C^1 values that produce a bound H-dibaryon. But the coupling between the channels generates a sizeable effective attraction which increases when the channel thresholds come closer. The dashed curve is a calculation with the contact term C^1 fixed to simulate the binding energy (-13.2 MeV) of the NPLQCD Collaboration at $M_\pi = 389$ MeV. As one can see, the dependence of the binding energy on the Σ mass is rather similar. The curve is simply shifted downwards by around 4.5 MeV, i.e. by the difference in the binding energy observed already at the physical masses. The asterisks and crosses represent results where, besides the variation of the $\Sigma\Sigma$ threshold, the ΞN threshold is shifted to coincide with that of the $\Lambda\Lambda$ channel. This produces an additional increase of the H binding energy by 20 MeV at the physical $\Sigma\Sigma$ threshold and by 9 MeV for that case where all three BB threshold coincide. Altogether there is an increase in the binding energy of roughly 60 MeV when going from the physical point to the case of baryons with identical masses. This is significantly larger than the variations due to the pion mass considered before. Note that we have kept the pion mass at its physical value while varying the BB thresholds.

4.2. Comparison with lattice QCD results

After these exemplary studies let us now try to connect with the published H binding energies from the lattice QCD calculations [11,12]. The results obtained by the HAL QCD Collaboration are obviously for the SU(3) symmetric case and the corresponding masses are given in Table I of Ref. [12]. Thus, we can take those masses and then fix the LEC C^1 so that we reproduce their H binding energy with those masses. To be concrete: we use $M_{ps} = 673$ MeV and $m_B = 1485$ MeV, and fix C^1 so that $E_H = -35$ MeV. We denote this interaction by YY-HAL. When we now let the masses of the baryons and mesons go to their physical values the bound state moves up to the $\Lambda\Lambda$ threshold, crosses the threshold, crosses also the ΞN threshold and then disappears. In fact, qualitatively this outcome can be already read off from the curves in Fig. 3 by combining the effects from the variations in the pion and the baryon masses. Based on those results one expects a shift of the H binding energy in the order of 60 to 70 MeV for the mass parameters of the HAL QCD calculation.

In case of the NPLQCD calculation we take the values provided in Ref. [38], as before. Those yield then 17 MeV for the ΞN-$\Lambda\Lambda$ threshold separation (to be compared with the physical value of roughly 26 MeV) and 77 MeV for the $\Sigma\Sigma$-$\Lambda\Lambda$ separation (physical value around 154 MeV). We also use the meson masses of Ref. [38], specifically $M_\pi = 389$ MeV. With those baryon and meson masses we fix again the LEC C^1 so
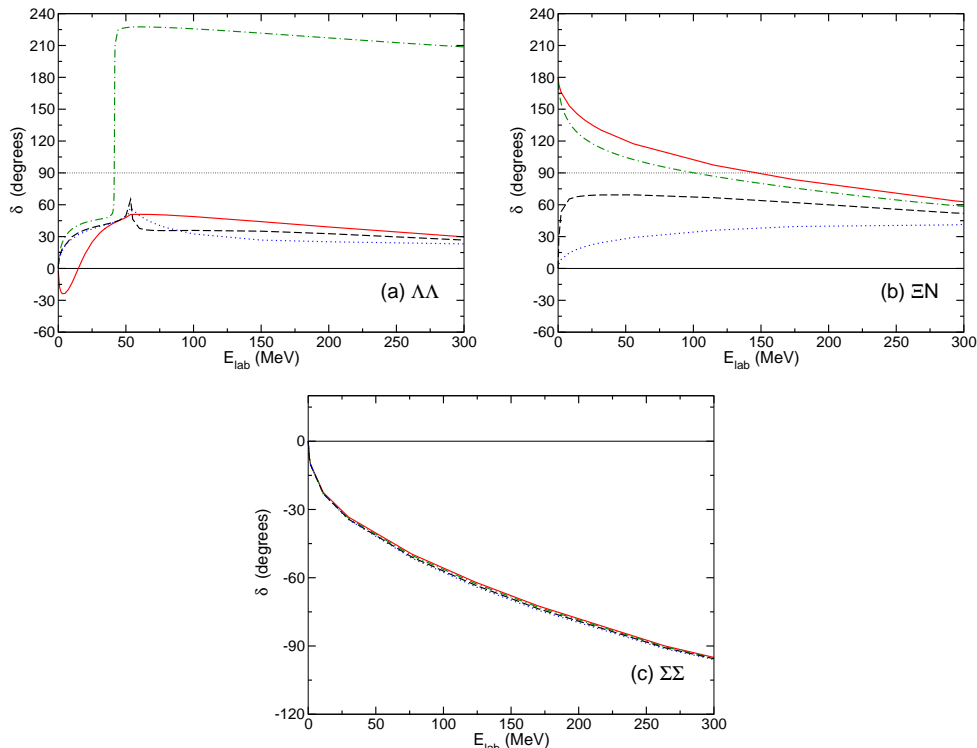
Fig. 4. Phase shifts in the $^1S_0$ partial wave in the $I = 0$ channel of $\Lambda\Lambda$ (a), ΞN (b) and $\Sigma\Sigma$ (c) as a function of the pertinent laboratory energies. The solid line is the result for our illustrative BB interaction that produces a bound H at $E_H = -1.87 \, \text{MeV}$. The dotted line corresponds to the EFT potential of Ref. [7] (Table 4) with cutoff mass $\Lambda = 550 \, \text{MeV}$. The other curves are results for interactions that are fine-tuned to the H binding energies found in the lattice QCD calculations of the HAL QCD (dashed) and NPLQCD (dash-dotted) Collaborations, respectively, for the pertinent meson (pion) and baryon masses as described in the text.

that we reproduce the H binding energy given by the NPLQCD Collaboration, namely $E_H = -13.2 \, \text{MeV}$ [11] (called YY-NPL in the following). Again we let the masses of the baryons and mesons approach their physical values. Also here the bound state moves up to and crosses the $\Lambda\Lambda$ threshold. However, in the NPLQCD case the state survives and remains below the ΞN threshold at the physical point. Specifically, we observe a resonance at a kinetic energy of 21 MeV in the $\Lambda\Lambda$ system or, more precisely, a quasi-bound state in the ΞN system around 5 MeV below its threshold.

It is interesting to observe that the chiral extrapolation of the lattice QCD results performed by Shanahan et al. [15] yields results that are qualitatively similar to ours. In that reference the authors conclude that the H-dibaryon is likely to be unbound by 13±14 MeV at the physical point. Let us emphasize, however, that our values are not really comparable with theirs. As said above, in our analysis we assume that the H-dibaryon is actually a bound BB state – which seems to be the case also in the lattice QCD studies [11,12]. On the other hand, in Ref. [15] it is assumed that the H is a compact, multi-quark state rather than a loosely bound molecular state, i.e. an object as originally suggested by Jaffe. How such a genuine multi-quark state would be influenced by variations of the BB thresholds is completely unclear. It depends, among other things, on whether and how strongly this state couples to the $\Lambda\Lambda$, ΞN, and $\Sigma\Sigma$ channels. So far there is no information on this issue from lattice QCD calculations. Clearly, in case of a strong and predominant coupling to the $\Lambda\Lambda$ alone, variations of the $\Sigma\Sigma$ and ΞN would not influence the H binding energy significantly. However, should it couple primarily to the ΞN and/or $\Sigma\Sigma$ channels then we expect a sensitivity of the binding energy to their thresholds values comparable to what we found in our study for the case of a bound state.

Phase shifts for the $^1S_0$ partial wave of the $\Lambda\Lambda$, ΞN and $\Sigma\Sigma$ channels are presented in Fig. 4. The solid line

is the result for the BB interaction YY-D that produces a loosely bound H dibaryon with $E_H = -1.87$ MeV. The phase shift for the ΞN channel, Fig. 4 (b), is rather similar to the one for the $^3S_1$ NN partial wave where the deuteron resides, see e.g. [31]. Specifically, it starts at 180°, decreases smoothly and eventually approaches zero for large energies, fulfilling the Levinson theorem. The result for $\Lambda\Lambda$ ($^1S_0$), Fig. 4 (a), behaves rather differently. This phase commences at zero degrees, is first negative but becomes positive within 20 MeV and finally turns to zero again for large energies. The dashed curve corresponds to the interaction YY-HAL that was fitted to the result of the HAL QCD Collaboration and reproduces their bound H dibaryon with their meson and baryon masses. The phase shift of the ΞN channel, calculated with physical masses, shows no trace of a bound state anymore. Still the phase shift rises up to around 60° near threshold, a behavior quite similar to that of the $^1S_0$ NN partial wave where there is a virtual state (also called antibound state [47,48]). Indeed, such a virtual state also seems to be present in the ΞN channel as a remnant of the original bound state. The effect of this virtual state can be seen in the $\Lambda\Lambda$ phase shift where it leads to an impressive cusp at the opening of the ΞN channel, cf. the dashed line in Fig. 4 (a).

In the ΞN phase shifts for the NPLQCD case (dash-dotted curve) the presence of a bound state is clearly visible. The corresponding $\Lambda\Lambda$ phase shift exhibits a resonance-like behavior at the energy where the (quasi-bound) H dibaryon is located.

The dotted curves are the results for the original chiral EFT potential with cut-off $\Lambda = 550$ MeV as published in [7]. The $\Lambda\Lambda$ as well as the ΞN phase shifts are qualitatively similar to the ones for the HAL QCD case. But the smaller ΞN phase shift together with the reduced cusp effect indicate that there is no near-by virtual state produced by this interaction.

The $\Sigma\Sigma$ phase shifts predicted by the various interactions are almost the same, cf. Fig. 4 (c). This may be not too surprising. After all, the $\Sigma\Sigma$ threshold is rather far away from the one of the $\Lambda\Lambda$ channel and the region, where we have introduced the H dibaryon. Thus, it remains practically unaffected by those changes.

Finally, for illustrative purposes, we present cross sections for the $\Lambda\Lambda$ and $\Xi^- p$ channels. Results of corresponding calculations, now performed in particle basis (but neglecting the Coulomb interaction), are displayed in Fig. 5. There are some experimental constraints for these two channels. In particular, there is an upper limit of 24 mb at 90% confidence level for elastic $\Xi^- p$ scattering, while for the $\Xi^- p \to \Lambda\Lambda$ cross section at $p_{\text{lab}} = 500$ MeV/c a value of $4.3^{+6.3}_{-2.7}$ mb was reported [20].

As obvious from Fig. 5, there are significant differences in the cross sections predicted by the YY interactions generated in the context of the H-dibaryon discussion – however, only at low momenta where no experimental information is at hand so far. Anyhow, those results suggest that a determination of the $\Xi^- p$ cross section at $p_{\text{lab}} \approx 200$ MeV/c, say, with reasonable errors would already put strong constraints on the H-dibaryon. In particular, situations where it is located close to the ΞN threshold – as at is the case in our simulations of the NPLQCD and HAL QCD results (dash-dotted and dashed curves, respectively) – could be ruled out. Distinguishing an actually (though loosely) bound H-dibaryon (solid curve) from the situation without any H-dibaryon (dotted curve) certainly requires better statistics. Here one has to keep in mind that the $\Xi^- p$ cross section would be even closer to the latter result, should the H-dibaryon be somewhat stronger bound than assumed in our calculation. Note that the peak in the $\Xi^- p$ cross section around 575 MeV/c is a cusp due to the opening of the $\Sigma^0\Lambda$ channel.

There are also characteristic differences in the predictions for $\Xi^- p \to \Lambda\Lambda$, cf. Fig. 5 (c). However, since this cross section rises to infinity with decreasing p_{lab}, due to the phase-space factor, it might be more difficult to draw conclusions in this case.

The assumed H dibaryon below the $\Lambda\Lambda$ threshold introduces a rather strong and peculiar energy variation in the near-threshold $\Lambda\Lambda$ cross section, cf. the solid curve in Fig. 5 (a). The effects due to the other considered interactions is less spectacular, specifically, because the structure produced by the NPLQCD case is so narrow that it would be presumably completely washed out once one takes into account the finite momentum resolution of an actual experiment. In any case, measuring the $\Lambda\Lambda$ cross section directly seems to be practically impossible. However, one could measure the $\Lambda\Lambda$ invariant mass spectrum in reactions like $K^- A \to \Lambda\Lambda + X$ where A can be the deuteron or a heavier nucleus. As a matter of facts, corresponding results from a measurement of K^{-12}C have been already published [9]. Still, it is unclear whether such an invariant mass distribution would be dominated by the $\Lambda\Lambda \to \Lambda\Lambda$ transition amplitude or rather by $\Xi N \to \Lambda\Lambda$. Since our investigation suggests that any near-threshold H-dibaryon will have a large if not
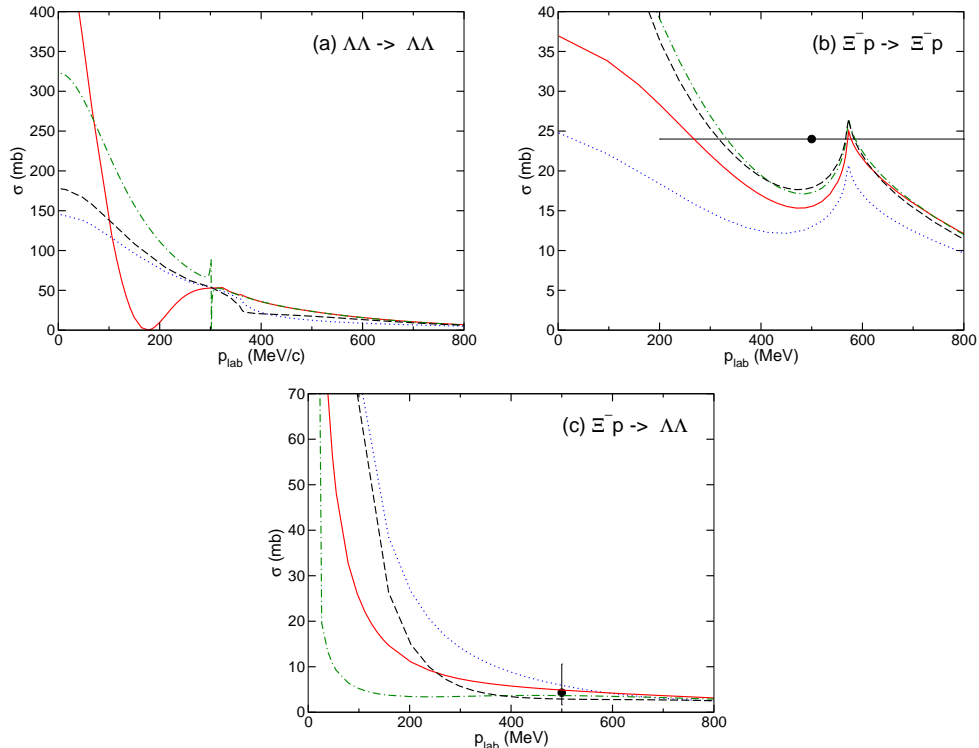
Fig. 5. Total cross sections for some $S = -2$ channels as a function of p_{lab}. The solid line is the result for our illustrative BB interaction that produces a bound H at $E_H = -1.87$ MeV. The dotted line corresponds to the EFT potential of Ref. [7] (Table 4) with cutoff mass $\Lambda = 550$ MeV. The other curves are results for interactions that are fine-tuned to the H binding energies found in the lattice QCD calculations of the HAL QCD (dashed) and NPLQCD (dash-dotted) Collaborations, respectively, for the pertinent meson (pion) and baryon masses as described in the text. The experimental cross sections in (b) and (c) are taken from Ref. [20].

dominant ΞN component one expects that then the $\Xi N \to \Lambda\Lambda$ amplitude should play likewise an important if not decisive role for the $\Lambda\Lambda$ invariant mass distribution.

5. Summary

In this paper we have presented an analysis of the quark mass dependence of binding energies for baryon-baryon systems in the strangeness $S = -2$, $S = -3$, and $S = -4$ sectors in the framework of chiral effective field theory at leading order in the Weinberg counting. In particular, we have explored the dependence of those binding energies on the pion mass in order to connect with current lattice QCD calculations. We remark that at higher orders, other effects like the quark mass dependence of the meson-baryon couplings or of the contact interactions will have to be considered (see e.g. [18]).

With regard to the $\Xi\Xi$, $\Xi\Sigma$ and $\Xi\Lambda$ systems, where meson-exchange potentials as well as leading-order EFT interactions, derived under the assumption of (broken) SU(3) symmetry, predict the existence of bound states in the various $^1S_0$ partial waves, we find a rather weak dependence of the binding energies on the pion mass. For the $\Xi^-\Xi^-$ system a calculation performed with meson and baryon masses that match the status of a recent lattice QCD exploration by the NPLQCD Collaboration yields binding energies that are compatible with the reported lattice QCD result [11] within the given error bars.

We have also investigated the situation concerning the so-called H-dibaryon. Here we found rather drastic effects caused by the SU(3) breaking related to the values of the three thresholds $\Lambda\Lambda$, $\Sigma\Sigma$ and ΞN. For physical values the binding energy of the H is reduced by as much as 60 MeV as compared to a calculation based on degenerate (i.e. SU(3) symmetric) BB thresholds. Translating this observation to the situation in

13

the HAL QCD [12] calculation, we see that the bound state has disappeared at the physical point. For the case of the NPLQCD calculation [11], a resonance in the $\Lambda\Lambda$ system might survive.

Acknowledgements

References

[1] R. L. Jaffe, Phys. Rev. Lett. **38**, 195 (1977) [Erratum-ibid. **38**, 617 (1977)].
[2] P. Adlarson *et al.* [WASA-at-COSY Collaboration], Phys. Rev. Lett. **106**, 242302 (2011).
[3] A. Gal, [arXiv:1011.6322 [nucl-th]].
[4] G. Miller, [arXiv:nucl-th/0607006].
[5] V. G. J. Stoks and T. A. Rijken, Phys. Rev. C **59**, 3009 (1999).
[6] H. Polinder, J. Haidenbauer, U.-G. Meißner, Nucl. Phys. A **779**, 244 (2006).
[7] H. Polinder, J. Haidenbauer, U.-G. Meißner, Phys. Lett. B **653**, 29 (2007).
[8] J. Haidenbauer, U.-G. Meißner, Phys. Lett. **B684**, 275 (2010).
[9] C.J. Yoon *et al.*, Phys. Rev. C **75**, 022201 (2007).
[10] S. R. Beane *et al.*, Phys. Rev. Lett. **106**, 162001 (2011).
[11] S. R. Beane *et al.*, [arXiv:1109.2889 [hep-lat]].
[12] T. Inoue *et al.*,, Phys. Rev. Lett. **106**, 162002 (2011).
[13] T. Inoue, [arXiv:1109.1620 [hep-lat]].
[14] S. R. Beane *et al.*, [arXiv:1103.2821 [hep-lat]].
[15] P. E. Shanahan, A. W. Thomas, R. D. Young, Phys. Rev. Lett. **107**, 092004 (2011).
[16] S. R. Beane, M. J. Savage, Nucl. Phys. A **713**, 148 (2003).
[17] S. R. Beane, M. J. Savage, Nucl. Phys. A **717**, 91 (2003).
[18] E. Epelbaum, U.-G. Meißner, W. Glöckle, Nucl. Phys. A **714**, 535 (2003).
[19] E. Epelbaum, U.-G. Meißner, W. Glöckle, [arXiv:nucl-th/0208040].
[20] J. K. Ahn *et al.*, Phys. Lett. B **633**, 214 (2006).
[21] J. Haidenbauer, U. -G. Meißner, Phys. Lett. B **706**, 100 (2011).
[22] J. Haidenbauer, U. -G. Meißner, A. Nogga, H. Polinder, Lect. Notes Phys. **724**, 113 (2007).
[23] M. J. Savage, M. B. Wise, Phys. Rev. D **53**, 349 (1996).
[24] C. L. Korpa, A. E. L. Dieperink, R. G. E. Timmermans, Phys. Rev. C **65**, 015208 (2002).
[25] S. R. Beane, P. F. Bedaque, A. Parreño, M. J. Savage, Nucl. Phys. A **747**, 55 (2005).
[26] J. J. de Swart, Rev. Mod. Phys. **35**, 916 (1963).
[27] C. B. Dover, H. Feshbach, Annals Phys. **217**, 51 (1992).
[28] P. G. Ratcliffe, Phys. Lett. B **365**, 383 (1996).
[29] T. Yamanishi, Phys. Rev. D **76**, 014006 (2007).
[30] E. Epelbaum, W. Glöckle, U.-G. Meißner, Nucl. Phys. A **637**, 107 (1998).
[31] E. Epelbaum, W. Glöckle, U.-G. Meißner, Nucl. Phys. A **747**, 362 (2005).
[32] H. Takahashi *et al.*, Phys. Rev. Lett. **87**, 212502 (2001).
[33] I. N. Filikhin, A. Gal, V. M. Suslov, Phys. Rev. C **68**, 024002 (2003).
[34] T. A. Rijken, Y. Yamamoto, Phys. Rev. C **73**, 044008 (2006).
[35] Y. Fujiwara, Y. Suzuki, C. Nakamoto, Prog. Part. Nucl. Phys. **58**, 439 (2007).
[36] A.M. Gasparyan, J. Haidenbauer, C. Hanhart, [arXiv:1111.0513 [nucl-th]].
[37] M. Frink, U.-G. Meißner, I. Scheller, Eur. Phys. J. **A24** , 395 (2005).
[38] S. R. Beane et al., Phys. Rev. D **84**, 014507 (2011).
[39] J. Schaffner-Bielich, R. Mattiello and H. Sorge, Phys. Rev. Lett. **84**, 4305 (2000).
[40] J. Steinheimer, M. Mitrovski, T. Schuster, H. Petersen, M. Bleicher, H. Stöcker, Phys. Lett. B **676**, 126 (2009).
[41] J. Schwinger, Phys. Rev. **72**, 742 (1947).
[42] H. A. Bethe, Phys. Rev. **76**, 38 (1949).
[43] M. Oka, K. Shimizu, K. Yazaki, Phys. Lett. **130B**, 365 (1983).
[44] C. Nakamoto, Y. Suzuki, Y. Fujiwara, Prog. Theor. Phys. **97**, 761 (1997).
[45] J. Haidenbauer, U.-G. Meißner, Phys. Rev. C **72**, 044005 (2005).

[46] J. Haidenbauer, G. Krein, U.-G. Meißner, L. Tolos, Eur. Phys. J. A **47**, 18 (2011).

[47] A. M. Badalyan, L. P. Kok, M. I. Polikarpov, Yu. A. Simonov, Phys. Rept. **82**, 31 (1982).

[48] B. C. Pearce, B. F. Gibson, Phys. Rev. C **40**, 902 (1989).